

Tuning “kappticity” of tripodal ligands†

Dawn M. Friesen,^a Owen J. Bowles,^a Robert McDonald^{a,b} and Lisa Rosenberg^{*a}

Received 15th November 2005, Accepted 23rd March 2006

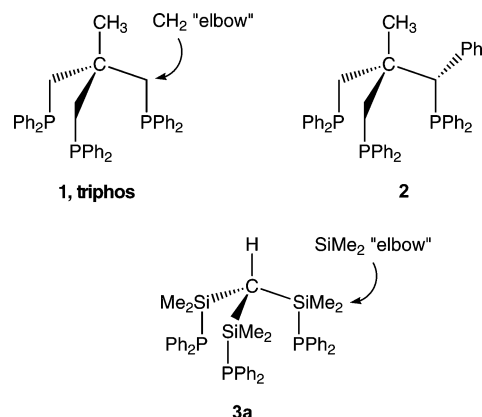
First published as an Advance Article on the web 6th April 2006

DOI: 10.1039/b516127d

The synthesis and structural characterization of a series of tripodal tris(phosphine) ligands, containing SiMe₂ elbow groups, is described. The significant steric congestion in these ligands, due to the silylmethyl substituents, is manifest both in the solid-state structures and in the solution NMR spectra of the free ligands. Variable temperature ¹H{³¹P} NMR studies of one of the ligands, CH₃C(SiMe₂PEt₂)₃ (**4b**) gave an estimated barrier to rotation around the Si–C_{apical} bonds of approximately 10.4 kcal mol⁻¹. Octahedral κ²- and κ³-molybdenum complexes of these ligands also demonstrate the impact of the additional bulk imparted by the SiMe₂ substituents, and the high Lewis basicity of these phosphines, with subtle changes at the apical and phosphine substituents changing the overall coordination chemistry observed.

Introduction

Multidentate phosphine ligands play an important role in transition metal coordination chemistry and catalysis.¹ Among these multifunctional, chelating ligands, tripodal tris(phosphine) compounds such as triphos (1,1,1-tris(diphenylphosphino)methyl)ethane, **1**)² have been exhaustively exploited and studied,^{1,3} due to the significant control they can offer over coordination environments at a metal centre, by anchoring three ancillary phosphine groups in mutually *cis* positions on one face of the metal. Considerable effort has been devoted to tailoring this useful ligand structure for a wide range of applications: tris(phosphine) tripods have been prepared with modified apical groups,⁴ apical pendant groups,⁵ and pendant substituents at phosphorus.⁶ However, the only examples of tripodal polyphosphines with other than –CH₂– groups *α* to phosphorus in the chelate backbone are compounds **2**⁷ and **3a**,^{8,9} and the potential impact of such modified elbow groups on the coordination chemistry of tripodal tris(phosphine) ligands remains relatively unexplored. Also, despite the prevalence of triphos-derived ligands in coordination chemistry, relatively few complexes of this popular tripodal framework with dialkyl substituents at phosphorus have been reported. We present here the synthesis and characterization of a series of tripodal tris(phosphine) ligands containing SiMe₂ elbow groups, including both Ph and Et substituents at phosphorus, and an evaluation of the electronic and steric properties of these bulky triphos analogues based on their molybdenum coordination chemistry.



Results

Ligand synthesis and characterization

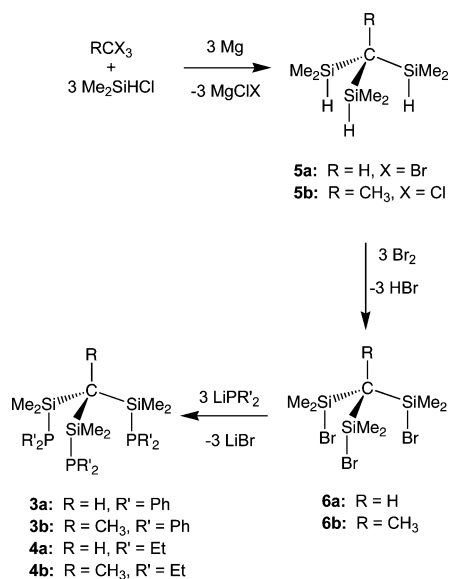
Bulky triphos analogs **3a–b** and **4a–b** were prepared as outlined in Scheme 1. 1,1,1-Tris(dimethylsilyl)ethane (**5b**) was not previously described in the literature, despite its structural similarity to the core of carbon-based triphos, CH₃C(CH₂PPh₂)₃ (**1**). The Si–Br bonds in **6a–b** were substituted by three equivalents of lithium diphenyl- or diethylphosphide to give compounds **3a–b** and **4a–b** in good yield.¹⁰

Fig. 1 and 2 show molecular structures determined for crystals of the methyl-capped tripods **6b** and **3b** (see Table 1 for selected bond lengths and angles). A key feature of the solid-state structures of H-capped tripods **6a** and **3a** is a widening and flattening of the tripodal trisilylmethane core, in particular relative to the solid-state structure of HC(CH₂PPh₂)₃,¹¹ which complements tripod conformation in minimizing interactions between silylmethyl elbow groups on adjacent arms of the tripods.⁹ However, solid-state structures of the Me-capped tripods **6b** (Br-substituted) and **3b** (PPh₂-substituted) do not exhibit this “splaying”, despite the presence of the SiMe₂ elbows. The average Si–C_{apical}–Si angles in **6b** and **3b** are both 110.6°, and, accordingly, the central carbon in these Me-capped tripods is approximately 0.2 Å further from

^aDepartment of Chemistry, University of Victoria, P.O. Box 3065, Victoria, British Columbia, Canada V8W 3V6. E-mail: lisarose@uvic.ca; Fax: 250-721-7147; Tel: 1-250-721-7173

^bX-Ray Crystallography Laboratory, Department of Chemistry, University of Alberta, Edmonton, Alberta, Canada T6G 2G2

† Electronic supplementary information (ESI) available: Experimental details including the solvolytic and oxidative sensitivities of **3** and **4** and the mechanism of phosphine exchange in **3b**. See DOI: 10.1039/b516127d



Scheme 1

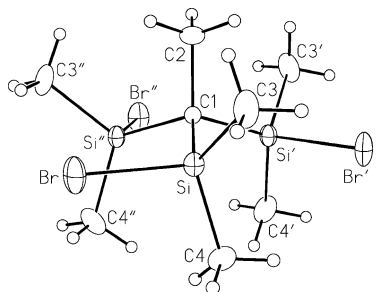


Fig. 1 Molecular structure of $\text{CH}_3\text{C}(\text{Me}_2\text{SiBr})_3$, **6b**. Shown is one of two enantiomeric forms, present in equal abundance in the crystal lattice.

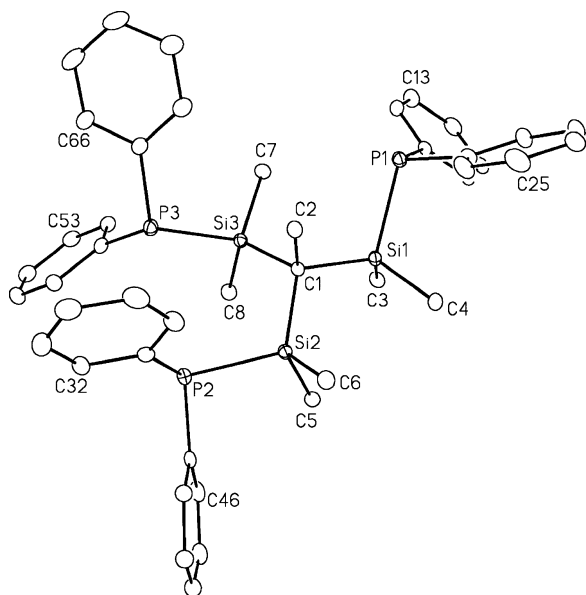


Fig. 2 Molecular structure of $\text{CH}_3\text{C}(\text{SiMe}_2\text{PPh}_2)_3$, **3b**.

the plane containing the three silicon atoms than in **6a** and **3a**: 0.600(7) Å in **6b** and 0.602(2) Å in **3b**. Thus the repulsions between $\text{H}_{\text{Me}(\text{apical})}$ and H_{SiMe} in methyl-capped **6b** and **3b** do not allow

distortion of the tetrahedral core. The resulting crowding renders the relative conformations of tripod arms in the methyl-capped compounds more sensitive than those in the corresponding H-capped tripods to the size of the non-methyl substituents at silicon, *i.e.* H, Br, PEt_2 , PPh_2 . For example, the solid-state structure of methyl-capped, Br-substituted tripod **6b** has a threefold rotation axis coincident with the apical $\text{CH}_3\text{-C}$ bond (Fig. 1, symmetry operations are given in footnote *a* of Table 1). One methyl group on each silicon elbow in **6b** points down toward the base of the tripod, approximately *anti* to the apical $\text{CH}_3\text{-C}$ bond, while the second methyl group points back toward the bromine atom on an adjacent arm. This “gearing” of the silyl methyl groups around the threefold central axis minimizes the interactions of these groups both with each other and with the apical methyl substituent. The H-capped, Br-substituted tripod **6a** adopts a more relaxed, unsymmetric, *syn-anti-anti* conformation, but an analogous, geared, C_3 -symmetric structure is observed for the H-capped tripod **3a**, with its larger PPh_2 -substituents.^{9a} Meanwhile, for the Me-capped, PPh_2 -substituted tripod **3b**, gearing of SiMe groups and bulky PPh_2 substituents is not sufficient to offset interactions between these groups and the methyl group at the apex of this tetrahedral Si_3 tripod. Dihedral angles of -42° , -46° , and 85° between the apical methyl carbon and the three phosphorus atoms in C_1 -symmetric **3b** give rise to the slightly “staggered” structure illustrated in Fig. 3. Two of the diphenylphosphine

Table 1 Selected bond lengths and angles for Me-capped tripods **6b** and **3b**

6b , $\text{CH}_3\text{C}(\text{SiMe}_2\text{Br})_3$		3b , $\text{CH}_3\text{C}(\text{SiMe}_2\text{PPh}_2)_3$	
Bond lengths/Å			
C1–C2	1.577(11)	C1–C2	1.567(3)
C1–Si	1.905(2)	C1–Si1	1.923(2)
		C1–Si2	1.911(2)
		C1–Si3	1.918(2)
Si–Br	2.2670(10)	Si1–P1	2.3151(9)
		Si2–P2	2.2948(9)
		Si3–P3	2.3063(9)
Si–C3	1.890(6)	Si1–C3	1.874(3)
Si–C4	1.814(7)	Si1–C4	1.871(3)
		Si2–C5	1.868(3)
		Si2–C6	1.882(2)
		Si3–C7	1.870(2)
		Si3–C8	1.872(2)
Bond angles/ $^\circ$			
Si–C1–Si'	110.6(2)	Si1–C1–Si2	110.03(11)
		Si1–C1–Si3	109.69(11)
		Si2–C1–Si3	112.09(11)
Br–Si–C1	109.38(5)	P1–Si1–C1	107.60(7)
		P2–Si2–C1	112.26(7)
		P3–Si3–C1	107.77(7)
Br–Si–C3	103.60(18)	C11–P1–C21	104.64(11)
		C31–P2–C41	101.34(11)
		C51–P3–C61	101.32(11)
Torsional angles/ $^\circ$			
Br–Si–C1–C2	83.29(8)	P1–Si1–C1–C2	$-42.07(15)$
		P2–Si2–C1–C2	$85.41(15)$
		P3–Si3–C1–C2	$-46.50(15)$

^a Primed atoms are related to unprimed ones *via* the rotational symmetry operation $(1 - y, x - y, z)$; double-primed atoms are related to unprimed ones *via* the operation $(1 - x + y, 1 - x, z)$ (both operations represent opposite-handed one-third rotations about the crystallographic threefold rotational axis $(2/3, 1/3, z)$).

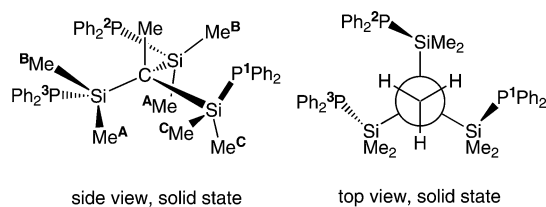


Fig. 3 Views illustrating C_1 symmetry and the distinct environments for SiMe groups in the molecular structure of **3b**.

substituents in **3b** (P^1 and P^3) are canted in the same direction (counter-clockwise), while the third phosphine fragment (P^2) has the opposite cant (clockwise). This arrangement distinguishes P^1 by placing it in a relatively unhindered environment, with the phenyl groups pointing out and away from the bulk of the tripod core. The remaining phosphine substituents (P^2 , P^3) are canted towards each other, which alleviates the crowding of SiMe₂ groups on these two arms of the tripod, with a partial “gearing” of the four phenyl groups, similar to that seen for **3a**. For the arms bearing P^2 and P^3 , one methyl group on each silicon atom is *anti* relative to the CH₃–C bond (Me^A), while the second methyl group is approximately *gauche* (Me^B). The SiMe groups on the third tripod arm (Me^C) are staggered between those on the other two arms, which optimizes the distance between the methyl and phenyl substituents. Silicon-phosphorus bond lengths in **3b** are 1–2% longer than those in **3a**, which is also consistent with the increased congestion around the core of **3b**. ³¹P{¹H} NMR spectra of **3b** in *d*₈-toluene at low temperature are consistent with a ground state solution structure analogous to this solid-state structure (see Electronic Supporting Information (ESI) for details).[†]

Also sensitive to the combined steric influence of substituents at the tripod apex and elbows are the barriers to tripod arm rotation around the C_{apical}–Si bonds for these compounds in solution, as illustrated in Scheme 2. While ¹H NMR spectroscopy of H-capped tripod **6a** (Br-derivative) shows a sharp singlet for the SiMe₂ protons even when the sample is cooled to 183 K, consistent with rapid arm rotation, the SiMe₂ signal in the ¹H NMR of compound **6b** (Me-capped, Br-derivative) in toluene-*d*₈ shows some broadening when the sample is cooled, which suggests that simply replacing the apical hydrogen in **6a** with a methyl group increases the barrier to rotation around the tripod

arms. The increase is not large enough to allow resolution of non-equivalent chemical shifts for distinct SiMe groups at low temperature (183 K). Low temperature ¹H NMR spectra of the H-capped, PET₂-substituted tripod **4a** show slight broadening of the SiMe₂ signal similar to that observed for **6b**, while the SiMe₂ signal for Me-capped, PET₂-substituted **4b** decoalesces into two broad singlets of equal intensity, similar to the decoalescence previously observed for H-capped, PPh₂-substituted **3a**,^{9a} consistent with slow exchange of SiMe groups between two inequivalent sites, in a ground state solution structure of pseudo-C₃ symmetry. Rotation around the C_{apical}–Si bonds is required for this exchange of SiMe groups, and the barrier to this rotation was determined by line-shape analysis of the SiMe peaks in the ¹H{³¹P} NMR spectra recorded for **4b** at low temperature (Fig. 4). An energy of activation (*E*_a) of 10.7 kcal mol⁻¹ for this two-site exchange is similar to that for **3a** (*E*_a = 10.9 kcal mol⁻¹),^{9a} which contains the smaller apical group (H) but larger PPh₂-substituents. Finally, the SiMe₂ signal in the ¹H{³¹P} NMR for a cooled sample of methyl-capped, PPh₂-substituted **3b** undergoes an apparent decoalescence at 195 K giving three broad singlets, consistent with a ground state

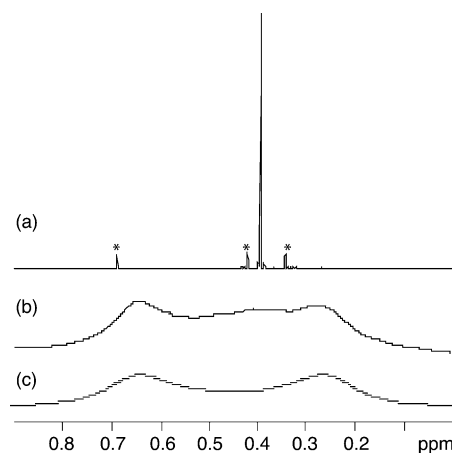
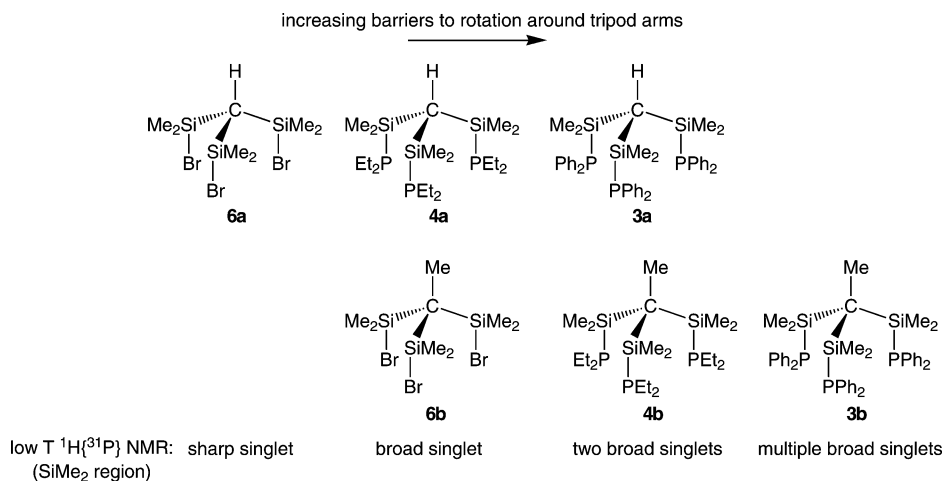


Fig. 4 The SiMe₂ region of (a) room temperature and (b) low temperature ¹H{³¹P} NMR spectra of CH₃C(SiMe₂PEt₂)₃, **4b**, in *d*₈-toluene. (c) Calculated low temperature spectrum. The vertical scale for (b) and (c) is 40× that for (a). Signals due to an impurity of the disubstituted compound CH₃C(Si(CH₃)₂Br){Si(CH₃)₂PEt₂}₂ are marked with “***”.



Scheme 2

solution structure of low symmetry, not inconsistent with its solid-state structure.¹²

Molybdenum carbonyl complexes of the tris(phosphine) tripods

The κ^2 -complexes **8a–b** and **9a–b** formed readily from the addition of ligands **3a–b** and **4a–b**, respectively, to $\text{Mo}(\text{pip})_2(\text{CO})_4$ (pip = piperidine) (eqn (1)), and were isolated as pale yellow solids, after removal of the solvent and free piperidine under vacuum. The $^{31}\text{P}\{^1\text{H}\}$ NMR spectra for all four κ^2 -complexes show two singlets in an approximately 2 : 1 ratio, with the shift of the lower intensity peaks corresponding closely to that for free tripod. The solid-state structure of **8a** (Fig. 5, bond distances and angles in Table 2) illustrates an approximate chair conformation adopted by the six member chelate ring, as anticipated for these κ^2 -molybdenum complexes.¹³

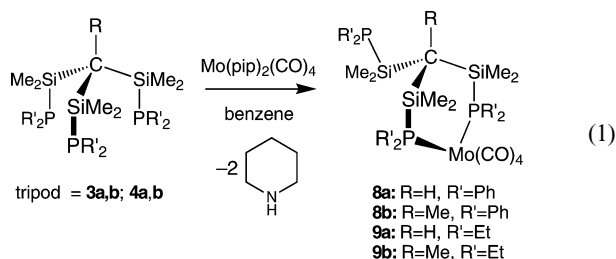


Table 2 Selected bond lengths and angles for **8a**, **10a**, and **10b**

8a: (κ^2 - 3a) $\text{Mo}(\text{CO})_4$		10a^a: (κ^3 - 4a) $\text{Mo}(\text{CO})_3$		10b: (κ^3 - 4b) $\text{Mo}(\text{CO})_3$	
Bond lengths/Å					
Mo–P1	2.5473(5)	Mo–P	2.5582(5)	Mo–P1	2.5577(4)
Mo–P2	2.5497(5)			Mo–P2	2.5554(4)
P1–Si1	2.3022(7)			Mo–P3	2.5547(4)
P2–Si2	2.3103(7)	SiA–P	2.3245(8)	Si1–P1	2.2947(5)
P3–Si3	2.2772(8)	SiB–P	2.277(3)	Si2–P2	2.2923(5)
Mo–C1	1.986(2)			Si3–P3	2.2979(6)
Mo–C2	1.973(2)	Mo–C1	1.955(2)	Mo–C1	1.9604(16)
Mo–C3	2.032(2)			Mo–C2	1.9550(16)
Mo–C4	2.031(2)			Mo–C3	1.9657(16)
Si1–C10	1.8981(19)	SiA–C10	1.8886(9)	Si1–C4	1.9028(16)
Si2–C10	1.8890(19)	SiB–C10	1.909(3)	Si2–C4	1.9103(16)
Si3–C10	1.9162(19)			Si3–C4	1.9028(16)
Bond angles/°					
P1–Mo–P2	91.109(16)	P–Mo–P'	90.388(15)	P1–Mo–P2	91.964(12)
				P1–Mo–P3	90.251(12)
				P2–Mo–P3	89.236(12)
Si1–C10–Si2	118.02(10)	SiA–C10–SiA'	114.98(7)	Si1–C4–Si2	112.42(7)
Si1–C10–Si3	110.58(9)	SiB–C10–SiB'	112.45(11)	Si1–C4–Si3	113.51(8)
Si2–C10–Si3	112.38(10)			Si2–C4–Si3	112.74(8)
Mo–P1–Si1	119.11(2)	Mo–P–SiA	116.33(2)	Mo–P1–Si1	117.360(18)
Mo–P2–Si2	124.24(2)	Mo–P–SiB	113.77(7)	Mo–P2–Si2	116.676(18)
				Mo–P3–Si3	116.390(18)
C11–P1–C21	99.47(9)	C11–P1–C13	100.92(10)	C11–P1–C13	101.23(8)
C31–P2–C41	103.56(9)			C21–P2–C23	100.94(7)
C51–P3–C61	106.37(10)			C31–P3–C33	100.96(8)
Torsional angles/°					
P1–Si1–C10–H	55.8	P–SiA–C10–H	–169.5	P1–Si1–C4–C5	–170.08(9)
P2–Si2–C10–H	–65.5	P–SiB–C10–H	159.8	P2–Si2–C4–C5	–166.58(10)
P2–Si3–C10–H	22.9			P3–Si3–C4–C5	–168.36(9)

^a While the solid-state structure of **10a** is highly symmetric, there is some disorder in the crystals. The SiA and SiB labels represent alternate atom positions arising from the presence of a tripod with an opposite “twist”. Atoms bearing an “A” label are refined at 5/6 occupancy, and “B” atoms are refined at 1/6 occupancy giving a local 5 : 1 disorder. However, due to the presence of an inversion center in the unit cell (centrosymmetric space group *R3*), the 5 : 1 disorder also occurs as a 1 : 5 disorder in the invertomer, resulting in an overall equal distribution of the tripod “hands”.

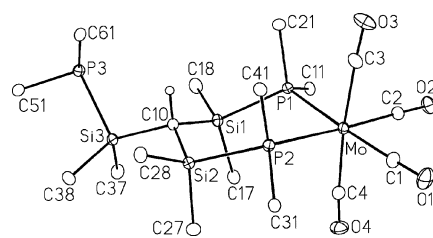
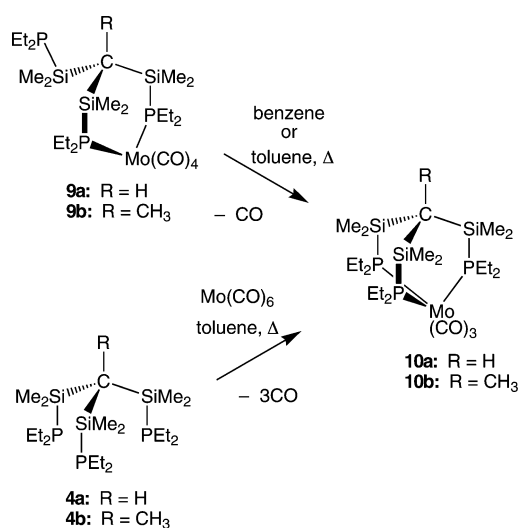


Fig. 5 Molecular structure of $\{\kappa^2\text{-HC}(\text{SiMe}_2\text{PPh}_2)_3\}\text{Mo}(\text{CO})_4$ (**8a**) showing the chair conformation of the six member chelate ring. Non-hydrogen atoms are represented by Gaussian ellipsoids at the 20% probability level. The hydrogen atom attached to the methyne carbon (C10) is shown with an arbitrarily small thermal parameter; all other hydrogens are not shown. For clarity, only the *ipso* carbons from the phenyl groups are shown.

As shown in Scheme 3, the κ^2 -complexes **9a–b**, containing PEt_2 -substituted ligands, convert to the corresponding κ^3 -complexes **10a–b**, with loss of one equivalent of CO, with heating in benzene or toluene. Complexes **10a–b** were isolated from the reactions of ligands **4a** and **4b** with $\text{Mo}(\text{CO})_6$ or $\text{Mo}(\eta^6\text{-mesitylene})(\text{CO})_3$ in refluxing toluene. The $^{31}\text{P}\{^1\text{H}\}$ NMR spectra of these κ^3 -complexes each show a singlet, surrounded by a low intensity sextet arising from coupling of the three equivalent phosphorus nuclei to ^{95}Mo ($I = 5/2$, 15.72% natural abundance, $^1J_{\text{Mo-P}} \approx 111$ Hz in both complexes). The molecular structures of **10a–b** are shown in



Scheme 3

Fig. 6 and 7, respectively, and relevant bond lengths and angles are listed in Table 2. Despite the conformational constraints imposed by coordination of all three bulky tripod arms in these complexes (*vide infra*), the geometry at Mo is undistorted octahedral, with chelate bite angles of approximately 90° . Reactions of **8a–b** or **3a–b** analogous to those shown in Scheme 3 did *not* give κ^3 -complexes of the PPh_2 -substituted ligands **3a–b**, even after prolonged reflux of reaction mixtures in toluene.¹⁴

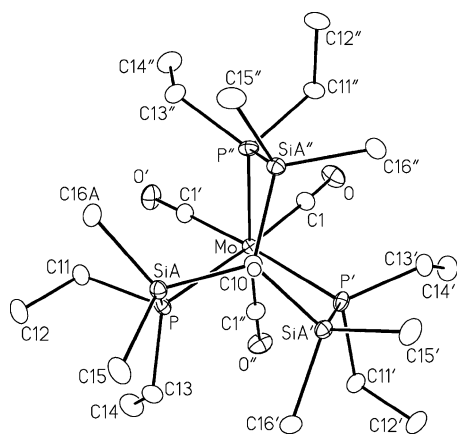


Fig. 6 View of the $\{\kappa^3\text{-HC}(\text{SiMe}_2\text{PEt}_2)_3\}\text{Mo}(\text{CO})_3$ molecule (**10a**) slightly offset along the C10–H bond axis, illustrating crystallographically imposed threefold symmetry. Atoms marked with a prime (') character are at $(-y, x - y, z)$ and those marked with a double prime (') are at $(-x + y, -x, z)$.

Discussion

Carbonyl stretching frequencies in the infrared spectra of the molybdenum carbonyl phosphine complexes **8–10** (see Table 3) apparently point to strong Lewis basicity of the ligands **3–4**. In particular, the κ^3 -tripodal complexes **10a–b** exhibit significantly lower stretching frequencies than is observed for a wide range of tris(phosphine) analogs (entries 1–2, 4–9 in Table 3), indicating a weaker CO bond due to increased back-bonding from molybdenum to CO. We have not found infrared data for κ^2 -

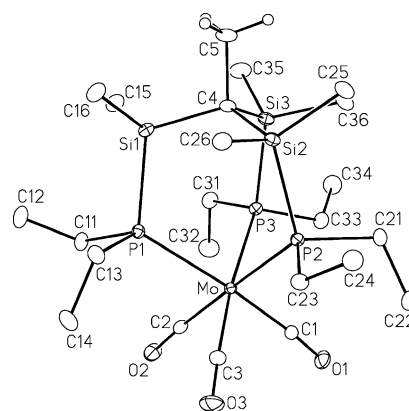
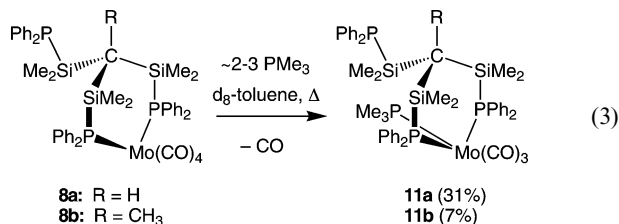
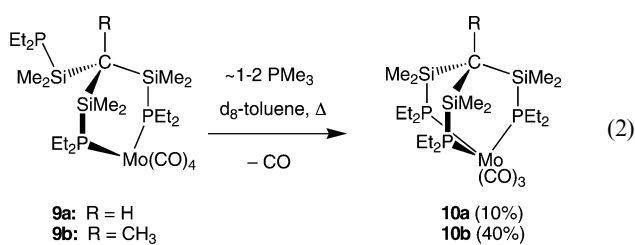


Fig. 7 Molecular structure of $\{\kappa^3\text{-CH}_3\text{C}(\text{SiMe}_2\text{PEt}_2)_3\}\text{Mo}(\text{CO})_3$ (**10b**).

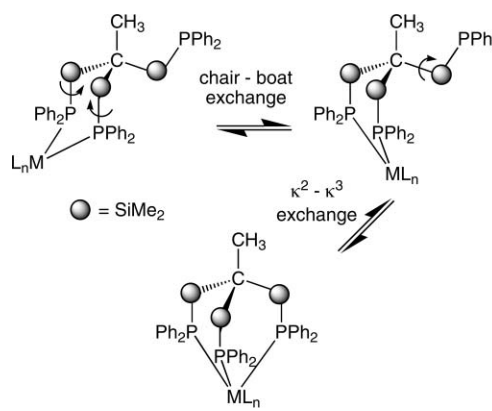
coordinated triphos ligands on molybdenum carbonyl fragments, but we note that ν_{CO} values for our κ^2 -complexes **8–9** are also consistently lower than those recorded for $(\text{R}_3\text{P})_2\text{Mo}(\text{CO})_4$ with $\text{R} = \text{Et}$ or Ph , respectively (entries 13–18). Among the few examples of tris(phosphine) molybdenum complexes exhibiting ν_{CO} close to those observed for **10a–b** are a series of κ^3 -triphosphacyclododecane complexes (*e.g.* entry 10), with all-alkyl substituents at each phosphorus,¹⁹ and a complex containing the very bulky phosphine $\text{P}\{\text{(H)NPr}^i\}_3$ (entry 3). This latter ligand, which is probably a good π -acid, should *limit* back-bonding to the carbonyl ligands, yet the carbonyl stretching frequencies are consistent with strong back-bonding from this P_3 molybdenum fragment. We note the much larger P–Mo–P angles of 94° in this complex: although the strongly donating SiMe_2 elbow groups, in concert with the ethyl substituents at phosphorus in tripods **4a–b**, probably do render our tris(phosphine) ligands very strong σ donors, we cannot rule out the influence of differences in coordination geometries on our observed ν_{CO} values. For example, there is very little variation in ν_{CO} for κ^3 -triphos derivatives with a range of different substituents at phosphorus (entries 4–9), though we note each example contains at least one aryl group at phosphorus. However, available crystallographic data suggests these triphos ligands also routinely impose P–Mo–P angles $\leq 85^\circ$ in their κ^3 -complexes, while ligands **4a–b** give P–Mo–P angles of about 90° in complexes **10a–b**, and $\{\text{cyclo}(\text{Pr}^i\text{PC}_3\text{H}_6)_3\}$ (entry 10) imposes an average P–Mo–P angle of 88° . Finally, consistent with a high Lewis basicity of the PEt_2 -substituted tripod arms of **4a–b**, which should render both the tripod and the ancillary CO ligands more stable to ligand substitution, the κ^2 -complexes **9a–b** do not react with approximately equimolar amounts of PMe_3 , even after 12 h of heating at 85°C , as determined by $^{31}\text{P}\{^1\text{H}\}$ NMR spectroscopic monitoring of mixtures of these complexes with 1–2 equiv of PMe_3 in d_8 -toluene in sealed NMR tubes. The only reaction observed in these experiments is partial conversion of the κ^2 -complexes to κ^3 , with loss of CO (eqn (2)),²⁰ which also occurs with heating in the absence of PMe_3 (*vide supra*). Mixtures of the PPh_2 -substituted κ^2 -complexes **8a–b** and approximately 2–3 equiv of PMe_3 in d_8 -toluene in sealed NMR tubes showed, after 4 h of heating at 85°C , signals corresponding to small amounts of the products **11a–b**, resulting from substitution of one CO ligand by PMe_3 (eqn (3)), perhaps indicative of a slightly lower Lewis basicity of **3a–b** relative to **4a–b**.²¹



The SiMe₂ elbow groups in tripods **3** and **4** also present steric constraints that affect the relative stabilities of κ^2 - and κ^3 -complexes incorporating these ligands, more than for analogous complexes of tripods with CH₂ elbow groups. This is illustrated by the structure of the κ^2 -complex **8a** (Fig. 5), containing PPh₂-substituted, H-capped ligand **3a**. An unusually wide angle of 118° at the tripodal ligand apex (Si(1)–C(10)–Si(2)) in the chelate ring in **8a** indicates the distortion from tetrahedral required to accommodate approximately *gauche* conformations of SiMe₂ and PPh₂ groups on adjacent arms of the κ^2 -ligand, and the third, un-coordinated tripod arm is twisted well out of the way of the Mo coordination sphere. The κ^3 -coordination of **3** or **4** requires *anti* conformations of all three phosphorus donors with respect to the apical substituent (H or Me), which forces Si–Me elbow substituents on adjacent tripod arms to point directly at each other. This all-*anti* tripod conformation has been shown to be sterically disfavored for the H-capped free ligand **3a** and its brominated precursor **6a**,⁹ and our crystallographic and variable

temperature NMR data point to at least the same degree of congestion in **3b** and **6b**. The crystal structures of κ^3 -complexes **10a–b** (Fig. 6 and 7) show puckering in the 5-membered chelate rings, which helps offset the Si–Me interactions on adjacent arms, and P–Et conformations that direct half of the ethyl groups well away from the SiMe₂ groups, while the remaining ethyl groups intercalate between SiMe₂ groups on each arm. Replacement of ethyl groups on phosphorus with phenyl groups would clearly place more strain on these κ^3 -structures, particularly for the flatter, H-capped ligand **3a**, leading to less stable complexes.

Greater stability of κ^2 -complexes of the PPh₂-substituted ligands **3a–b** relative to their putative κ^3 -complexes may explain why we have not observed coordination of that final tripod arm to yield (κ^3 -**3**)Mo(CO)₃ complexes. However, particularly high barriers to rotation around tripod arms in ligands **3a–b**, as discussed above, may also influence the rates of formation of these κ^3 -complexes, which presumably occurs *via* the κ^2 -complexes. As shown in Scheme 4, rotation around a Si–C_{apical} bond is required to pull



Scheme 4

Table 3 Infrared data for selected molybdenum carbonyl κ^3 phosphine complexes. Crystallographic data included where available

Entry	Complex	$\nu_{\text{CO}}/\text{cm}^{-1}$	P–Mo–P avg/°	C–Mo–C avg/°	Ref.
	<i>fac</i> -L ₃ Mo(CO) ₃ where L ₃ is:				
1	(PPh ₃) ₃	1934, 1835			15
2	(PEt ₃) ₃	1937, 1841			15
3	{P(N(H)Pr ⁱ) ₃ } ₃	1918, 1815	94	87	16
4	κ^3 -CH ₃ C(CH ₂ PPh ₂) ₃	1937, 1844	84	85	CH ₂ Cl ₂ ^{6b}
5	κ^3 -CH ₃ C(CH ₂ P(Et)Ph) ₃	1931, 1844	83	89	CH ₂ Cl ₂ ^{6b}
6	κ^3 -CH ₃ C(CH ₂ P(CH ₂ Ph)Ph) ₃	1934, 1838	83	87	CH ₂ Cl ₂ ^{6b}
7	κ^3 -CH ₃ C(CH ₂ P(4-tBuPh) ₂) ₃	1934, 1840			CH ₂ Cl ₂ ¹⁷
8	κ^3 -HOCH ₂ C(CH ₂ PPh ₂) ₃	1937, 1845			CH ₂ Cl ₂ ^{5c}
9	κ^3 -MeSO ₂ OCH ₂ C(CH ₂ PPh ₂) ₃	1927, 1844, 1826			CH ₂ Cl ₂ ^{5c}
10	κ^3 -{ <i>cyclo</i> -(Pr ⁱ PC ₃ H ₆) ₃ }	1915, 1813	88	87	18
11	κ^3 -HC(SiMe ₂ PEt ₂) ₃ (10a)	1904, 1802, 1773 (sh)	90	86	This work
12	κ^3 -CH ₃ C(SiMe ₂ PEt ₂) ₃ (10b)	1911, 1816, 1802	90	86	This work
	<i>cis</i> -L ₂ Mo(CO) ₄ where L ₂ is:				
13	(PPh ₃) ₂	2023, 1929, 1911, 1899			15
14	(PEt ₃) ₂	2016, 1915, 1900, 1890			15
15	κ^2 -HC(SiMe ₂ PPh ₂) ₃ (8a)	2015, 1917, 1876 (br)	91	89	This work ^a
16	κ^2 -CH ₃ C(SiMe ₂ PPh ₂) ₃ (8b)	2010, 1909, 1883, 1871			This work
17	κ^2 -HC(SiMe ₂ PEt ₂) ₃ (9a)	2002, 1892, 1881, 1859			This work
18	κ^2 -CH ₃ C(SiMe ₂ PEt ₂) ₃ (9b)	2005, 1881 (br), 1857			This work

^a These deviate somewhat from previously reported values of 1818, 1950(sh), 1925, 1880 cm⁻¹.⁸ In particular, we see no stretch at 1950 cm⁻¹. We note that the elemental analysis reported in reference 8 for this complex is 6.4% low in carbon. It may be that this sample contained some Mo–CO impurities.

the unbound tripod arm into the metal's coordination sphere. Perhaps even more importantly, the 6-membered metallacycle of the κ^2 -precursor must undergo a chair to boat conformational change before the phosphine on the third arm can coordinate to the metal. This involves Si–P bond rotations that may be significantly hindered by the SiMe₂ and PPh₂ interactions. Of course, these kinetic barriers to chair–boat inversion and single arm rotation should also render κ^3 -complexes of elbow-substituted tripods such as **3** and **4** considerably inert to arm-dissociation reactions, as is perhaps demonstrated by the lack of reaction of **10a–b** with PMe₃ (eqn (3)).

Conclusion

The silylmethyl elbow substituents in tripodal tridentate phosphine ligands **3** and **4** provide sufficient bulk to render tripod conformations extremely sensitive to variations in the size of the apical and phosphorus substituents. The presence of strongly donating silicon groups α - to phosphorus significantly enhances the Lewis basicity of these phosphines. Both of these features influence the molybdenum coordination chemistry of ligands **3** and **4**: our studies suggest that there is delicate energetic and kinetic balance between κ^2 and κ^3 coordination of these bulky ligands.

Experimental

General conditions, reagents, and instruments

Unless otherwise noted, all reactions and manipulations were performed under nitrogen in an MBraun Unilab 1200/780 glovebox or using conventional Schlenk techniques. Toluene was dried by distillation from sodium under argon; benzene, pentane, hexanes, tetrahydrofuran, and ether were distilled from sodium/benzophenone under argon. Deuterated solvents were purchased from Canadian Isotope Labs (CIL), freeze–pump–thaw degassed and vacuum transferred from over sodium/benzophenone (benzene-*d*₆, toluene-*d*₈) or calcium hydride (chloroform-*d*₁) before use. Chlorodimethylsilane, 1,1,1-trichloroethane, bromine, triphenylphosphine oxide, and *n*-butyllithium (1.6 M in hexanes) were purchased from Aldrich Chemical Co. and used as received without further purification. [AgI·PMe₃]₄ was purchased from Acros Chemical Co. and used as received. Diphenyl- and diethylphosphine were purchased from Strem Chemicals as 10 wt% solutions in hexanes, and the concentration checked against a known quantity of triphenylphosphine oxide by ³¹P{¹H} NMR before use. Tris(dimethylsilyl)methane (**5a**),²² tris(bromodimethylsilyl)methane (**6a**),^{9a,22} tris(diphenylphosphinodimethylsilyl)methane (**3a**),^{9a} (η^6 -mesitylene)tricarbonylmolybdenum(0)²³ and bis(piperidyl)tetracarbonylmolybdenum(0)²⁴ were prepared according to literature methods. Lithium diphenylphosphide and lithium diethylphosphide were prepared by the reaction of equimolar amounts of *n*-butyllithium and the desired dialkylphosphine in hexanes. NMR spectra were acquired on a Bruker AC 300 operating at 300.133 MHz for ¹H, and 75.469 MHz for ¹³C; a Bruker AMX 360 operating at 360.13 MHz for ¹H, 90.565 MHz for ¹³C, 145.784 MHz for ³¹P, and 71.550 MHz for ²⁹Si; a Bruker Avance 500 operating at 500.133 MHz for ¹H, 202.430 MHz for ³¹P, and 99.361 MHz for ²⁹Si. Chemical shifts

are reported in ppm at ambient temperature unless otherwise stated. ¹H chemical shifts are referenced to residual protonated solvent peaks at 7.15 ppm (C₆D₅H), 2.09 ppm (PhCD₂H), and 7.24 (CHCl₃). ¹³C chemical shifts are referenced to C₆D₆ at 128.4 ppm and CDCl₃ at 77.5 ppm. ¹H, ¹³C, and ²⁹Si chemical shifts are reported relative to tetramethylsilane, ³¹P chemical shifts are reported relative to 85% H₃PO₄(aq). Microanalysis was performed by Canadian Microanalytical Service Ltd., Delta, BC, Canada. IR spectra were recorded on a Perkin Elmer FTIR Spectrum 1000 spectrophotometer using KBr pellets (unless otherwise noted). Mass spectrometry was carried out by Mr David McGillivray in the Department of Chemistry, University of Victoria, and by Mr Wayne Buchannon in the Department of Chemistry, University of Manitoba.

Preparation of ligands

Synthesis of CH₃C(SiMe₂H)₃ (5b**).** Under a flow of nitrogen, magnesium powder (10.9 g, 0.450 mol) and THF (anhydrous, 150 mL) were stirred together in a 500 mL two-necked RB flask equipped with a magnetic stir bar, reflux condenser, and pressure equalizing dropping funnel. Chlorodimethylsilane (50 mL, 0.450 mol) was added to the RB flask by syringe. 1,1,1-Trichloroethane (15 mL, 0.150 mol) in THF (50 mL) was placed in the dropping funnel and added to the RB flask over a period of 2 h, with the dropping rate adjusted to maintain gentle reflux during the addition. The reaction mixture was stirred under reflux for an additional 4 h, then cooled to room temperature, poured over 500 mL crushed ice and allowed to stand for 1 h, then stirred for an additional hour. The mixture was filtered through glass wool into a 500 mL separatory funnel and the aqueous and organic layers separated. The aqueous layer was extracted with 2 × 30 mL of hexanes, and the organic layer washed with 2 × 30 mL of distilled water. The combined organic fractions were dried over MgSO₄, and then gravity filtered to remove the drying agent. Solvents were removed on a rotary evaporator, and the remaining liquid was distilled under reduced pressure. The fraction distilling between 60–80 °C (10 mmHg) was collected, giving **5b** as a clear oil in ≥97% purity.²⁵ Yield: 13.9 g (45%). ¹H NMR (300 MHz, C₆D₆, δ): 4.137 (sept, ³J_{HH} = 3.7 Hz, SiH), 1.071 (s, 3H, CCH₃), 0.129 (d, ³J_{HH} = 3.7 Hz, 18H, SiCH₃). ¹³C{¹H} NMR (75 MHz, C₆D₆, δ): 13.56 (s, CCH₃), –3.95 (s, SiCH₃), –5.54 (s, CCH₃). ²⁹Si{¹H} NMR (99 MHz, C₆D₆, δ): –9.20 (s, SiCH₃). IR (thin film on NaCl plate, cm^{–1}): 2103 ($\nu_{\text{Si-H}}$). MS (EI, 70 eV) *m/z*: 203 ([M – H], 7%), 189 ([M – CH₃], 32%), 144 ([M – Si(CH₃)₂H], 100%), 129 ([M – Si(CH₃)₃H], 81%), 85 ([M – 2Si(CH₃)₂H], 21%), 73 ([Si(CH₃)₃], 65%), 59 ([Si(CH₃)₂H], 74%), 40 ([SiC], 78%).

Synthesis of CH₃C(SiMe₂Br)₃ (6b**).** To a 500 mL three-neck round bottom flask equipped with a magnetic stir bar, pressure equalizing dropping funnel and two gas inlet adapters was added **5b** (10.50 g, 51.34 mmol) in benzene (20 mL). A 3.0 M solution of bromine (0.15 mol, 7.9 mL Br₂ total) in benzene was added dropwise over 2.5 h to the contents of the round bottom flask. A stream of nitrogen was passed through the flask and allowed to exit *via* a dispersion tube submerged in a 1 M solution of *cis*-cyclooctene in toluene (400 mL), then through a 1 cm layer of NaOH pellets, to trap product HBr(g) and any unreacted Br₂(g).

Once addition of bromine was complete, the mixture was allowed to stir for 30 min. The solvent was removed *in vacuo* to give a pale orange solid, which was purified by sublimation under vacuum with the aid of a heat gun to give a white crystalline solid. Yield: 18.19 g (80.3%). The product was resublimed (77 °C, 5×10^{-3} mmHg) to obtain a sample for elemental analysis. Mp (uncorrected) 225 °C (sublimes). ^1H NMR (300 MHz, C_6D_6 , δ): 1.091 (s, 3H, CCH_3), 0.689 (s, 18H, SiCH_3). $^{13}\text{C}\{^1\text{H}\}$ NMR (75 MHz, C_6D_6 , δ): 14.6 (s, CCH_3), 10.3 (s, CCH_3), 5.8 (s, SiCH_3). $^{29}\text{Si}\{^1\text{H}\}$ NMR (71 MHz, C_6D_6 , δ): 28.4 (s, SiCH_3). Anal. Calcd for $\text{C}_8\text{H}_{21}\text{Br}_3\text{Si}_3$: C 21.78, H 4.80. Found: C 21.85, H 4.75. MS (EI, 70 eV) m/z : 427 ([M – CH_3], 32%), 361 ([M – Br], 100%), 224 ([M – Br, $\text{Si}(\text{CH}_3)_2\text{Br}$], 61%), 139 ([$\text{Si}(\text{CH}_3)_2\text{Br}$], 21%), 85 ([M – Br, 2 $\text{Si}(\text{CH}_3)_2\text{Br}$], 38%), 73 ([$\text{Si}(\text{CH}_3)_3$], 37%).

Synthesis of $\text{HC}(\text{SiMe}_2\text{PEt}_2)_3$ (4a). In a Schlenk tube equipped with a magnetic stir bar, **6a** (1.49 g, 3.48 mmol) was dissolved in 3 mL THF and cooled in an ice bath. In a second Schlenk tube, LiPEt_2 (0.98 g, 10 mmol) was dissolved in THF (25 mL), and slowly added to the cooled solution of **6a** by cannula. After the LiPEt_2 addition was complete, the ice bath was removed, and the mixture allowed to stir under nitrogen. After 1.5 h, the solvent was removed under vacuum to give a pale yellow paste. The paste was extracted with dry hexanes (30 mL) and filtered by cannula; the solvent was removed from the filtrate under vacuum. The cloudy, pale yellow oil was dissolved in pentane (6 mL) and filtered through Celite to remove remaining solid LiBr . Pentane was removed under vacuum to give **4a** as a pale yellow oil in >95% purity.²⁶ Yield: 1.17 g (76%). ^1H NMR (360 MHz, C_6D_6 , δ): 1.56 (m, 6 H, PCH_2CH_3), 1.43 (m, 6 H, PCH_2CH_3), 1.18 (dt, $^3J_{\text{PH}} = 15.1$ Hz, $^3J_{\text{HH}} = 7.6$ Hz, 18 H, PCH_2CH_3), 0.47 (s, 18 H, SiCH_3), -0.12 (q, $^3J_{\text{PH}} = 3.9$ Hz, 1H, HCSi_3). $^{13}\text{C}\{^1\text{H}\}$ NMR (90 MHz, C_6D_6 , δ): 15.2 (m, PCH_2CH_3), 14.0 (m, PCH_2CH_3), 1.1 (q, $^2J_{\text{CP}} = 12.4$ Hz, HCSi_3), 1.0 (m, SiCH_3). $^{31}\text{P}\{^1\text{H}\}$ NMR (145 MHz, C_6D_6 , δ): -80.2 (s, PEt_2). $^{29}\text{Si}\{^1\text{H}\}$ NMR (99 MHz, C_6D_6 , δ): 2.56 (complex m, SiCH_3). MS (EI, 70 eV) m/z : 425 ([M – Et], 100%), 365 ([M – PEt_2], 72%), 275 ([M – 2PEt_2], 20%), 187 ([M – 3PEt_2], 12%).

Synthesis of $\text{CH}_3\text{C}(\text{SiMe}_2\text{PPh}_2)_3$ (3b). In a Schlenk tube equipped with a magnetic stir bar, LiPPh_2 (2.613 g, 13.60 mmol) was dissolved in 25 mL THF to give a clear red solution. A solution of **6b** (1.996 g, 4.524 mmol) in 5 mL THF was added to the LiPPh_2 solution by syringe, and stirred overnight under nitrogen. The solvent was removed under vacuum to give an orange paste, which was extracted with toluene (25 mL) and filtered by cannula to remove lithium bromide. Toluene was removed under vacuum to leave a yellow foam, which was washed with 3×10 mL dry pentane to give the product as a white powder. This was collected on a glass frit and dried under vacuum. Yield 2.86 g (83%). Mp (uncorrected) 166–168 °C. ^1H NMR (360 MHz, C_6D_6 , δ): 7.68 (m, 12 H, *o*- C_6H_5), 7.04 (br m, 18 H, *p*-, *m*- C_6H_5), 2.05 (s, 3H, CCH_3), 0.43 (br s, 18 H, SiCH_3). $^{13}\text{C}\{^1\text{H}\}$ NMR (90 MHz, C_6D_6 , δ): 136.9 (m, C_{ipso}), 135.4 (m, C_{ortho}), 128.1 (m, C_{meta}), 127.7 (s, C_{para}), 19.6 (q, $^3J_{\text{CP}} = 7.8$ Hz, CCH_3), 5.0 (q, $^2J_{\text{CP}} = 12.7$ Hz, CCH_3), 1.4 (td, $^4J_{\text{CP}} = 4.3$ Hz, $^2J_{\text{CP}} = 4.6$ Hz, SiCH_3). $^{31}\text{P}\{^1\text{H}\}$ NMR (145 MHz, C_6D_6 , δ): -50.9 (s, PPh_2). $^{29}\text{Si}\{^1\text{H}\}$ NMR (99 MHz, C_7D_8 , δ): 8.28 (complex m, SiCH_3). Anal. Calcd for $\text{C}_{44}\text{H}_{51}\text{P}_3\text{Si}_3$: C 69.81, H 6.79;

Found: C 67.82, H 6.72.²⁷ MS (EI, 70 eV) m/z : 571 ([M – PPh_2], 11%), 386 ([M – 2PPh_2], 11%), 201 ([M – 3PPh_2], 19%).

Synthesis of $\text{CH}_3\text{C}(\text{SiMe}_2\text{PEt}_2)_3$ (4b). In a Schlenk tube equipped with a magnetic stir bar, **6b** (1.62 g, 3.67 mmol) was dissolved in 3 mL THF and cooled in an ice bath. In a second Schlenk tube, LiPEt_2 (1.01 g, 10.6 mmol) was dissolved in THF (25 mL), and slowly added to the cooled solution of **6b** by cannula. After the LiPEt_2 addition was complete, the ice bath was removed, and the mixture was allowed to stir under nitrogen. After 1 h, the solvent was removed under vacuum to give a yellow paste. The paste was extracted with dry hexanes (25 mL) and filtered by cannula; the solvent was removed from the filtrate under vacuum. The cloudy, pale yellow oil was dissolved in pentane (6 mL) and filtered through Celite to remove remaining solid LiBr . Pentane was removed under vacuum to give **4b** as a yellow oil in >95% purity (by ^1H NMR).²⁶ Yield: 1.44 g (87%). Bp > 130 °C (5×10^{-3} mmHg). ^1H NMR (360 MHz, C_6D_6 , δ): 1.63 (m, 6 H, PCH_2CH_3), 1.41 (s, 3H, CCH_3), 1.40 (m, 6 H, PCH_2CH_3), 1.19 (dt, $^3J_{\text{PH}} = 15.1$ Hz, $^3J_{\text{HH}} = 7.6$ Hz, 18 H, PCH_2CH_3), 0.41 (s, 18 H, SiCH_3). $^{13}\text{C}\{^1\text{H}\}$ NMR (90 MHz, C_6D_6 , δ): 16.8 (q, $^3J_{\text{CP}} = 8.6$ Hz, CCH_3), 15.6 (m, PCH_2CH_3), 14.3 (m, PCH_2CH_3), 2.9 (q, $^2J_{\text{CP}} = 11.9$ Hz, $\text{C}(\text{CH}_3)$), -0.5 (td, $^4J_{\text{CP}} = 4.2$ Hz, $^3J_{\text{CP}} = 3.7$ Hz, SiCH_3). $^{31}\text{P}\{^1\text{H}\}$ NMR (145 MHz, C_6D_6 , δ): -81.4 (s, PEt_2). $^{29}\text{Si}\{^1\text{H}\}$ NMR (99 MHz, C_6D_6 , δ): 6.65 (complex m, SiCH_3). MS (EI, 70 eV) m/z : 439 ([M – Et], 70%), 379 ([M – PEt_2], 68%), 321 ([M – $\text{SiMe}_2\text{PEt}_2$], 14%), 291 ([M – 2PEt_2], 14%). For the disubstituted tripod $\text{CH}_3\text{C}(\text{SiMe}_2\text{PEt}_2)_2(\text{SiMe}_2\text{Br})$: ^1H NMR (360 MHz, C_6D_6 , δ): 1.65–1.50 (m, 6 H, PCH_2CH_3), 1.45–1.30 (m, 6 H, PCH_2CH_3), 1.33 (s, 3H, CCH_3), 1.20–1.10 (m, 18 H, PCH_2CH_3), 0.71 (s, 6 H, SiCH_3Br), 0.44 (br s, 6 H, $\text{SiCH}_3\text{PEt}_2$), 0.35 (br s, 6 H, $\text{SiCH}_3\text{PEt}_2$). $^{31}\text{P}\{^1\text{H}\}$ NMR (145 MHz, C_6D_6 , δ): -82.6 (s, PEt_2).

Preparation of molybdenum complexes

Synthesis of $\kappa^2\text{-(HC}(\text{SiMe}_2\text{PPh}_2)_3\text{)Mo}(\text{CO})_4$ (8a). Compound **3a** (0.51 g, 0.68 mmol) and $\text{Mo}(\text{pip})_2(\text{CO})_4$ (0.26 g, 0.68 mmol) were suspended in 30 mL dry toluene in a Schlenk tube. The headspace was evacuated and the yellow suspension stirred under static vacuum in an oil bath for 2 h at 45 °C, after which the solvent was removed *in vacuo*. The resulting sticky golden brown foam was washed with hexanes (10 mL), and the washings were decanted by cannula filtration to give **8a** as a pale yellow powder that was dried under vacuum. Yield: 0.32 g (49%). Spectroscopic and physical properties are in agreement with those reported in the literature.⁸

Synthesis of $\kappa^2\text{-(CH}_3\text{C}(\text{SiMe}_2\text{PPh}_2)_3\text{)Mo}(\text{CO})_4$ (8b). This compound was prepared as described above for compound **8a**, using the following reagents and amounts: compound **3b** (0.40 g, 0.53 mmol), $\text{Mo}(\text{pip})_2(\text{CO})_4$ (0.20 g, 0.51 mmol), 25 mL benzene. Yield: 0.33 g (69%).²⁸ Mp 125 °C (decomp). ^1H NMR (360 MHz, CDCl_3 , δ): 7.59 (m, 4H, *o*- $\text{C}_6\text{H}_5\text{PMo}$), 7.52 (m, 4H, *o*- $\text{C}_6\text{H}_5\text{PMo}$), 7.41 (m, 4H, *o*- $\text{C}_6\text{H}_5\text{P}$), 7.4–7.2 (m, 18H, *p*-, *m*- $\text{C}_6\text{H}_5\text{P/PMo}$), 1.36 (br s, 3H, CCH_3), 0.48 (d, $^3J_{\text{PH}} = 2.9$ Hz, 6H, SiCH_3), 0.45 (d, $^3J_{\text{PH}} = 6.1$ Hz, 6H, SiCH_3PMo), 0.14 (d, $^3J_{\text{PH}} = 2.5$ Hz, 6H, MoPSiCH_3). $^{13}\text{C}\{^1\text{H}\}$ NMR (90 MHz, CDCl_3 , δ): 215.2 (dd, $^2J_{\text{CP}(\text{trans})} = 23.1$ Hz, $^2J_{\text{CP}(\text{cis})} = 9.1$ Hz, CO), 214.7 (t, $^2J_{\text{CP}(\text{cis})} = 7.1$ Hz, CO), 208.4 (t, $^2J_{\text{CP}(\text{cis})} = 7.2$ Hz, CO), 137.5 (dd,

$^1J_{CP} = 21.1$ Hz, $^3J_{CP} = 6.8$ Hz, *ipso*-C₆H₅PMo), 137.3 (d, $^1J_{CP} = 21.7$ Hz, *ipso*-C₆H₅PMo), 135.1 (d, $^2J_{CP} = 20.7$ Hz, *o*-C₆H₅PMo), 135.1 (d, $^1J_{CP} = 13.1$ Hz, *ipso*-C₆H₅P), 135.0 (d, $^2J_{CP} = 12.1$ Hz, *o*-C₆H₅PMo), 134.0 (d, $^2J_{CP} = 11.4$ Hz, *o*-C₆H₅P), 128.8 (s, *p*-C₆H₅P), 128.4 (s, *p*-C₆H₅P), 128.4 (d, $^3J_{CP} = 7.1$ Hz, *m*-C₆H₅P), 128.1 (s, *p*-C₆H₅P), 128.1 (d, $^3J_{CP} = 6.7$ Hz, *m*-C₆H₅P), 128.0 (d, $^3J_{CP} = 7.5$ Hz, *m*-C₆H₅P), 18.6 (d, $^3J_{CP} = 10.0$ Hz, CCH₃), 8.0 (d, $^2J_{CP} = 9.1$ Hz, CCH₃), 3.6 (d, $^2J_{CP} = 11.7$ Hz, SiCH₃PMo), 2.1 (d, $^2J_{CP} = 5.8$ Hz, SiCH₃PMo), 0.7 (d, $^2J_{CP} = 10.0$ Hz, SiCH₃). $^{31}\text{P}\{^1\text{H}\}$ NMR (145 MHz, CDCl₃, δ): -18.9 (s, 2P, PMo), -50.4 (s, 1P, P). $^{29}\text{Si}\{^1\text{H}\}$ NMR (99 MHz, C₆D₆, δ): 7.66 (dt, $^1J_{SiP} = 40.4$ Hz, $^3J_{SiP} = 8.1$ Hz, 1Si, SiP_{free}), 7.14 (m, 2Si, SiPMo). MS (FAB, *m*NBA matrix) *m/z*: 966 ([M], 2%), 782 ([M - PPh₂], 21%), 753 ([M - PPh₂, - CO], 40%), 725 ([M - PPh₂, - 2CO], 38%), 697 ([M - PPh₂, - 3CO], 68%), 669 ([M - PPh₂, - 4CO], 39%). IR (KBr disk, ν_{CO} , cm⁻¹): 2010 (s), 1909 (s), 1883 (s), 1871 (s).

Synthesis of κ^2 -(HC(SiMe₂PEt₂)₃)Mo(CO)₄ (9a). In a Schlenk tube, **4a** (0.43 g, 0.94 mmol) was dissolved in 30 mL dry toluene. Mo(pip)₂(CO)₄ (0.37 g, 0.97 mmol) was added under a flow of nitrogen, and the cloudy yellow suspension was allowed to stir at RT under static vacuum for four days, until all of the solid had dissolved to give a clear yellow solution. The solvent was removed *in vacuo* to give a pale yellow paste that was extracted into 10 mL hexanes and filtered by cannula. The hexanes was removed under vacuum, and the residue washed with 5 mL of ice cold pentane to give **9a** as a pale yellow powder which was dried under vacuum. Yield 0.32 g (51%). Mp 123–130 °C. ^1H NMR (360 MHz, C₆D₆, δ): 1.70–1.51 (overlapping m, 6H, PCH₂CH₃), 1.50–1.21 (overlapping m, 6H, PCH₂CH₃), 1.14–0.95 (overlapping m, 18H, PCH₂CH₃), 0.42 (d, $^3J_{PH} = 3.2$ Hz, 6H, SiCH₃(free)), 0.18 (d, $^3J_{PH} = 2.2$ Hz, 12H, SiCH₃(Mo)), 0.12 (dt, $^3J_{PH} = 3.6$ Hz, $^3J_{PH} = 1.8$ Hz, 1H, CH). $^{13}\text{C}\{^1\text{H}\}$ NMR (90 MHz, C₆D₆, δ): 216.1 (dd, $^2J_{CP(trans)} = 22.2$ Hz, $^2J_{CP(cis)} = 12.3$ Hz CO), 213.4 (t, $^2J_{CP(cis)} = 6.3$ Hz, CO), 211.8 (t, $^2J_{CP(cis)} = 9.5$ Hz, CO), 19.7 (dd, $^1J_{CP} = 11.3$ Hz, $^3J_{CP} = 8.0$ Hz, MoPCH₂CH₃), 19.1 (dd, $^1J_{CP} = 13.5$ Hz, $^3J_{CP} = 8.9$ Hz, MoPCH₂CH₃), 15.0 (d, $^1J_{CP} = 16.4$ Hz, PCH₂CH₃), 13.9 (d, $^2J_{CP} = 16.3$ Hz, PCH₂CH₃), 10.6 (s, MoPCH₂CH₃), 10.2 (s, MoPCH₂CH₃), 3.2 (dt, $^2J_{CP} = 11.0$ Hz, $^2J_{CP} = 9.6$ Hz, CH), 1.8 (d, $^2J_{CP} = 8.2$ Hz, SiCH₃), 1.4 (br s, SiCH₃), 0.3 (d, $^2J_{CP} = 4.4$ Hz, SiCH₃). $^{31}\text{P}\{^1\text{H}\}$ NMR (145 MHz, C₆D₆, δ): -49.3 (s, 2P, MoPEt₂), -81.2 (s, 1P, PEt₂). $^{29}\text{Si}\{^1\text{H}\}$ NMR (99 MHz, C₆D₆, δ): 1.91 (dt, $^1J_{SiP} = 29.8$ Hz, $^3J_{SiP} = 8.7$ Hz, 1Si, SiP_{free}), 0.03 (m, 2Si, SiPMo). MS (FAB, *m*NBA matrix) *m/z*: 592 ([M - SiMe₃], 18%), 564 ([M - SiMe₃, - CO], 11%), 536 ([M - SiMe₃, - 2CO], 36%), 508 ([M - SiMe₃, - 3CO], 92%), 506 ([M - (HCSiMe₂PEt₂)], 100%). IR (KBr disk, ν_{CO} , cm⁻¹): 2002 (s), 1883 (br s), 1859 (s).

Synthesis of κ^2 -(CH₃C(SiMe₂PEt₂)₃)Mo(CO)₄ (9b). This compound was prepared as described above for compound **9a**, using the following reagents and amounts: compound **4b** (0.55 g, 1.2 mmol), Mo(pip)₂(CO)₄ (0.45 g, 1.2 mmol), 30 mL toluene. Yield 0.32 g (41%) yellow powder, in $\geq 95\%$ purity (by ^1H NMR).²⁹ Mp 87–105 °C. ^1H NMR (360 MHz, C₆D₆, δ): 1.9–1.2 (overlapping m, 12H, PCH₂CH₃), 1.34 (s, CCH₃), 1.2–0.9 (overlapping m, 18H, PCH₂CH₃), 0.30 (d, $^3J_{HP} = 2.9$ Hz, 6H, SiCH₃), 0.27 (d, $^3J_{HP} = 4.3$ Hz, 6H, SiCH₃), 0.09 (d, $^3J_{HP} = 1.8$ Hz, 6H, SiCH₃). $^{13}\text{C}\{^1\text{H}\}$ NMR (90 MHz, C₆D₆, δ): 216.3 (dd, $^2J_{CP(trans)} = 20.1$ Hz, $^2J_{CP(cis)} = 10.9$ Hz, CO), 212.7 (t, $^2J_{CP(cis)} = 6.9$ Hz, C≡O), 211.9 (t, $^2J_{CP(cis)} =$

7.2 Hz, CO), 20.5 (br d, $^1J_{CP} = 15.5$ Hz, MoPCH₂CH₃), 18.5 (d, $^1J_{CP} = 14.2$ Hz, MoPCH₂CH₃), 16.1 (br d, $^3J_{CP} = 7.3$ Hz, CCH₃), 15.2 (d, $^1J_{CP} = 17.8$ Hz, PCH₂CH₃), 13.9 (d, $^2J_{CP} = 18.5$ Hz, PCH₂CH₃), 11.1 (s, MoPCH₂CH₃), 10.0 (s, MoPCH₂CH₃), 2.5 (m, CCH₃), 1.5 (br s, SiCH₃), -0.5 (d, $^2J_{CP} = 5.3$ Hz, SiCH₃), -1.0 (s, SiCH₃). $^{31}\text{P}\{^1\text{H}\}$ NMR (145 MHz, C₆D₆, δ): -55.5 (s, 2P, MoPEt₂), -78.5 (s, 1P, PEt₂). $^{29}\text{Si}\{^1\text{H}\}$ NMR (99 MHz, C₆D₆, δ): 5.64 (dt, $^1J_{SiP} = 29.8$ Hz, $^3J_{SiP} = 6.6$ Hz, 1Si, SiP_{free}), 2.95 (m, 2Si, SiPMo). MS (FAB, *m*NBA matrix) *m/z*: 648 ([M - EtH], 25%), 606 ([M - SiMe₃], 22%), 590 ([M - PEt₂], 22%), 578 ([M - SiMe₃, - CO], 26%), 550 ([M - SiMe₃, - 2CO], 61%), 522 ([M - SiMe₃, - 3CO], 100%), 506 ([M - (CH₃CSiMe₂PEt₂)], 28%). IR (KBr disk, ν_{CO} , cm⁻¹): 2005 (s), 1881 (br s), 1857 (s).

Synthesis of κ^3 -(HC(SiMe₂PEt₂)₃)Mo(CO)₃ (10a). This compound can be prepared from Mo(CO)₆ (method (a)) but we have obtained higher yields using Mo(mesitylene)(CO)₃ as a precursor (method (b)). *Method (a)*. Under a flow of nitrogen, a thick walled glass reaction vessel with a J. Young valve (100 mL capacity) was charged with a magnetic stir bar, Mo(CO)₆ (0.499 g, 1.90 mmol), HC(SiMe₂PEt₂)₃ (0.843 g, 1.85 mmol), and 30 mL dry toluene. The headspace was evacuated and the vessel sealed under static vacuum, then heated in an oil bath at 120 °C for 18 h. After cooling to room temperature, solvent was removed *in vacuo* to give a yellow paste, which was washed with hexanes (2 × 10 mL) to give κ^3 -[HC(SiMe₂PEt₂)₃]Mo(CO)₃ as a white powder that was isolated by filtration and dried under vacuum. Yield 0.267 g (22.7%). *Method (b)*. Under nitrogen, a 250 mL Schlenk flask was charged with **4a** (610 mg, 1.34 mmol), and Mo(mesitylene)(CO)₃ (402 mg, 1.34 mmol). Toluene (90 mL) was added by syringe, the flask was equipped with a reflux condenser, and the clear yellow solution was heated at reflux for 2 h. When the solution cooled, the solvent was removed under vacuum to leave a pale yellow solid. Repeated washing with hexanes (4 × 10 mL) and toluene (2 × 10 mL) ultimately allowed isolation of **10a** as a white microcrystalline powder, which was dried under vacuum. Yield 0.455 g (54%). Mp 220 °C (decomp). ^1H NMR (300 MHz, C₆D₆, δ): 1.90–1.70 (m, 12 H, PCH₂CH₃), 1.08 (dt, $^3J_{PH} = 13.5$ Hz, $^3J_{HH} = 7.3$ Hz, 18 H, PCH₂CH₃), 0.06 (br d, $^3J_{PH} = 1.9$ Hz, 18 H, SiCH₃), -1.01 (q, $^4J_{PH} = 16.2$ Hz, 1H, CH). $^{31}\text{P}\{^1\text{H}\}$ NMR (121 MHz, C₆D₆, δ): -56.9 (s, PEt₂), also see sext, $^1J_{95\text{Mo}31\text{P}} = 109$ Hz. Anal. Calcd for C₂₂H₄₀MoO₃P₃Si₃: C 41.63, H 7.78; Found: C 41.32, H 8.08. IR (KBr disk, ν_{CO} , cm⁻¹): 1904 (s), 1802 (s), 1773 (sh).

Synthesis of κ^3 -(CH₃C(SiMe₂PEt₂)₃)Mo(CO)₃ (10b). Under a flow of nitrogen, a thick walled glass reaction vessel with a Teflon J. Young valve (100 mL capacity) was charged with a magnetic stir bar, Mo(CO)₆ (0.999 g, 3.78 mmol), CH₃C(SiMe₂PEt₂)₃ (2.5 g, 3.8 mmol), and 30 mL dry toluene. The headspace was evacuated and the vessel sealed under static vacuum, then heated in an oil bath at 120 °C for 18 h. After the mixture was cooled to room temperature, solvent was removed *in vacuo* to give a yellow paste, which was washed with pentane (20 mL). A pale yellow powder was isolated by filtration, washed repeatedly with hexanes and toluene and dried under vacuum. Yield 0.80 g (33%). Mp 227 °C (decomp). ^1H NMR (360 MHz, C₆D₆, δ): 1.85 (m, 6 H, PCH₂CH₃), 1.76 (m, 6 H, PCH₂CH₃), 1.08 (dt, $^3J_{PH} = 13.3$ Hz, $^3J_{HH} = 7.4$ Hz, 18 H, PCH₂CH₃), 0.77 (q, $^4J_{PH} = 1.8$ Hz, 3H, CCH₃), 0.01 (d, $^3J_{PH} = 1.8$ Hz, 18 H, SiCH₃). $^{13}\text{C}\{^1\text{H}\}$ NMR (90 MHz, C₆D₆, δ): 220.7 (m, CO), 19.1 (m, PCH₂CH₃), 13.1 (q, $^3J_{CP} = 5.3$ Hz, CCH₃),

9.9 (s, $\omega_{1/2} \sim 5$ Hz, PCH_2CH_3), 2.6 (q, $^2J_{\text{CP}} = 16.6$ Hz, CCH_3), 0.2 (s, $\omega_{1/2} \sim 5$ Hz, SiCH_3). $^{31}\text{P}\{^1\text{H}\}$ NMR (145 MHz, C_6D_6 , δ): -57.3 (s, PEt_2), also see sext, $^1J_{95\text{Mo}31\text{P}} = 110.8$ Hz. $^{29}\text{Si}\{^1\text{H}\}$ NMR (99 MHz, C_6D_6 , δ): 2.16 (complex m, SiCH_3). Anal. Calcd for $\text{C}_{23}\text{H}_{51}\text{MoO}_3\text{P}_3\text{Si}_3$: C 42.58, H 7.92; Found: C 42.72, H 8.04. MS (FAB, *m*NBA matrix) *m/z*: 650 ($[\text{M}]$, 24%), 622 ($[\text{M} - \text{CO}]$, 46%), 594 ($[\text{M} - 2\text{CO}]$, 100%). IR (KBr disk, ν_{CO} , cm^{-1}): 1911, 1816, 1802.

Other reactions

Conversion of $\kappa^2\text{-(HC(SiMe}_2\text{PEt}_2)_3\text{)Mo(CO)}_4$ (9a**) to $\kappa^3\text{-(HC(SiMe}_2\text{PEt}_2)_3\text{)Mo(CO)}_3$ (**10a**).** Compound **9a** (9 mg, 0.01 mmol) was dissolved in 0.5 mL C_7D_8 in a 5 mm NMR tube equipped with a Teflon J. Young valve, and degassed by one freeze–pump–thaw cycle. The sample was heated in an oil bath at 85 °C and removed periodically to monitor the progress of reaction by $^{31}\text{P}\{^1\text{H}\}$ NMR spectroscopy. After 22.5 h, 38% of **9a** had converted to the κ^3 complex **10a**.

Conversion of $\kappa^2\text{-(CH}_3\text{C(SiMe}_2\text{PEt}_2)_3\text{)Mo(CO)}_4$ (9b**) to $\kappa^3\text{-(CH}_3\text{C(SiMe}_2\text{PEt}_2)_3\text{)Mo(CO)}_3$ (**10b**).** Compound **9b** (21 mg, 0.031 mmol) was dissolved in 0.5 mL C_7D_8 in a 5 mm NMR tube equipped with a Teflon J. Young valve, and degassed by one freeze–pump–thaw cycle. The sample was heated in an oil bath at 85 °C and removed periodically to monitor the progress of reaction by $^{31}\text{P}\{^1\text{H}\}$ NMR spectroscopy. After 12 h, 32% of **9b** had converted to the κ^3 complex **10b**.

Reactions of molybdenum tripod complexes with PMe_3 . Approximately 30 mg of the desired tripod–molybdenum complex was placed in a sealable NMR tube, and attached *via* a glass “T” connector to a 10 mL RB flask containing an appropriate amount of $[\text{AgI} \cdot \text{PMe}_3]_4$. The entire apparatus was connected to a vacuum line and placed under vacuum, and toluene- d_8 (0.5 mL) was vacuum transferred into the NMR tube. Under static vacuum, the NMR tube was cooled in liquid nitrogen, and the RB flask containing $[\text{AgI} \cdot \text{PMe}_3]_4$ was warmed with a heat gun until evolution of PMe_3 could no longer be observed. After allowing the PMe_3 to collect in the NMR tube, the tube was flame sealed under static vacuum, and warmed to room temperature. The actual amount of PMe_3 present in each tube was determined by $^{31}\text{P}\{^1\text{H}\}$ NMR, relative to the known amount of tripod–molybdenum complex (delay time $D1 = 20$ s). $^{31}\text{P}\{^1\text{H}\}$ NMR spectra were rerecorded after heating the tubes in an oil bath at 85 °C for 12–16 h. Percent conversions are reported with respect to the overall amount of tripodal ligand present in the sample.

Reaction of $\kappa^2\text{-(HC(SiMe}_2\text{PPh}_2)_3\text{)Mo(CO)}_4$ (8a**) with PMe_3 .** Compound **8a** (20 mg, 0.021 mmol), PMe_3 (0.039 mmol). After 12 h at 85 °C, $^{31}\text{P}\{^1\text{H}\}$ NMR showed **8a** ($\delta -21.4$ and -52.4 , $\sim 67\%$), $(\kappa^2\text{-HC}\{\text{SiMe}_2\text{PPh}_2\}_3\text{)(PMe}_3\text{)Mo(CO)}_3$ ($\delta -19.2$ d, -24.6 t, and -51.3 s, $\sim 31\%$), PMe_3 ($\delta -62.3$), and a small amount of HPPH_2 ($\delta -40.4$).

Reaction of $\kappa^2\text{-(CH}_3\text{C(SiMe}_2\text{PPh}_2)_3\text{)Mo(CO)}_4$ (8b**) with PMe_3 .** Compound **8b** (38 mg, 0.039 mmol), PMe_3 (0.10 mmol). After 12 h at 85 °C, $^{31}\text{P}\{^1\text{H}\}$ NMR showed **8b** ($\delta -17.9$ and -50.2 , $\sim 58\%$), $(\kappa^2\text{-CH}_3\text{C}\{\text{SiMe}_2\text{PPh}_2\}_3\text{)(PMe}_3\text{)Mo(CO)}_3$ ($\delta -13.7$ d, -23.7 t, and -49.3 s, $\sim 7\%$), $(\kappa^3\text{-CH}_3\text{C}\{\text{SiMe}_2\text{PPh}_2\}_3\text{)Mo(CO)}_3$,

free $\text{CH}_3\text{C}\{\text{SiMe}_2\text{PPh}_2\}_3$ ($\delta -50.9$, $\sim 25\%$), *cis*- $\text{Mo(PMe}_3)_2(\text{CO})_4$ ($\delta -16.4$), *trans*- $\text{Mo(PMe}_3)_2(\text{CO})_4$ ($\delta -6.3$), and PMe_3 ($\delta -62.3$), and signals due to an unidentified species ($\delta -17.5$).

Reaction of $\kappa^2\text{-(HC(SiMe}_2\text{PEt}_2)_3\text{)Mo(CO)}_4$ (9a**) with PMe_3 .** Compound **9a** (29 mg, 0.044 mmol), PMe_3 (0.038 mmol). After 12 h at 85 °C, $^{31}\text{P}\{^1\text{H}\}$ NMR showed only **9a** ($\delta -49.1$, -81.2), PMe_3 ($\delta -62.3$), and trace amounts of HPEt_2 ($\delta -55.6$). Small white crystals on the walls of the NMR tube were identified as **10a**, indicating that $\sim 10\%$ of the original complex had converted from κ^2 to κ^3 coordination, with concomitant liberation of CO.

Reaction of $\kappa^2\text{-(CH}_3\text{C(SiMe}_2\text{PEt}_2)_3\text{)Mo(CO)}_4$ (9b**) with PMe_3 .** Compound **9b** (28 mg, 0.041 mmol), PMe_3 (0.099 mmol). After 16 h at 85 °C, $^{31}\text{P}\{^1\text{H}\}$ NMR showed **9b** ($\delta -55.4$ and -78.6 , $\sim 60\%$), **10b** ($\delta -57.0$, $\sim 30\%$), PMe_3 ($\delta -62.3$), and trace amounts of HPEt_2 ($\delta -55.6$). Peaks potentially representing $\sim 15\%$ of the total tripod complex were also observed, but were unassigned ($\delta -54.8$ (s), -55.7 (s)).

Reaction of $\kappa^3\text{-(CH}_3\text{C(SiMe}_2\text{PEt}_2)_3\text{)Mo(CO)}_3$ (10b**) with PMe_3 .** Compound **10b** (32 mg, 0.049 mmol), PMe_3 (0.007 mmol). After 12 h at 85 °C, $^{31}\text{P}\{^1\text{H}\}$ NMR showed no change; only **10b** ($\delta -57.0$), and PMe_3 ($\delta -62.3$) were detected.

Line-shape analysis of **4b** and related calculations

Line-shape analysis was carried out on the SiMe region of $^1\text{H}\{^{31}\text{P}\}$ NMR (500 MHz) spectra recorded for compound **4b** in toluene- d_8 at 200, 195, 190, 185, and 180 K, using a modified version of DNMR3^{30a} contained in SpinWorks 2.3.^{30b} Rate constants (*k*) for the two-site exchange were determined iteratively at each temperature, giving well-matched simulated and experimental spectra. Estimated errors in *k* varied from 2–6%, temperatures are ± 5 K. Thermodynamic parameters were obtained from the slope and intercept of an Eyring plot ($\ln(k/T)$ vs. $1/T$, $R^2 = 0.9972$): $\Delta H^\ddagger = 10.4$ kcal mol $^{-1}$, $\Delta S^\ddagger = 10.9$ cal K mol $^{-1}$. These yielded $\Delta G^\ddagger(300\text{ K}) = 7.1$ kcal mol $^{-1} \pm 0.2$ kcal mol $^{-1}$ (2.8% error). Energy of activation, $E_a = 10.7$ kcal mol $^{-1}$, was determined from the slope of an Arrhenius plot ($\ln k$ vs. $1/T$, $R^2 = 0.9973$). ΔG^\ddagger was also calculated for decoalescence of the SiMe signals in the variable temperature $^1\text{H}\{^{31}\text{P}\}$ NMR spectra (500 MHz) recorded for compound **4b** using the value for the rate constant k_C (where $k_C = \pi\Delta\nu_C/(2)^{1/2}$) in the Eyring equation

$$\Delta G^\ddagger = -RT_C \ln[(k_C h)/(k_B T_C)],$$

where *R* = the gas constant, T_C = coalescence temperature, $\Delta\nu_C$ = peak separation at the low-temperature limit, *h* = Planck's constant, and k_B = Boltzmann constant. For the two-site exchange of SiMe groups in **4b**: $T_C = 184\text{ K} \pm 5\text{ K}$, $\Delta\nu_C = 218\text{ Hz}$, $\Delta G^\ddagger = 8.2 \pm 0.2$ kcal mol $^{-1}$.

X-Ray crystallographic studies

Single crystals suitable for X-ray diffraction were grown from hexanes (**6b**) or toluene (**3b**, **8a**, **10a–b**) solutions at -20 °C under nitrogen, and mounted on glass fibres in hydrocarbon oil. Selected crystal data and structural refinement details are listed in Table 4; further details are given in the ESI.†

CCDC reference numbers 289572–289576.

Table 4 Crystallographic experimental details

Compound	3b	6b	8a	10a	10b
Formula	C ₄₄ H ₅₁ P ₃ Si ₃	C ₈ H ₂₁ Br ₃ Si ₃	C ₅₄ H ₅₇ MoO ₄ P ₃ Si ₃	C ₂₃ H ₄₉ MoO ₃ P ₃ Si ₃	C ₂₃ H ₅₁ MoO ₃ P ₃ Si ₃
M_r	757.03	441.25	1043.12	634.73	648.76
Crystal size/mm	0.43 × 0.27 × 0.24	0.88 × 0.19 × 0.16	0.66 × 0.22 × 0.21	0.40 × 0.29 × 0.23	0.44 × 0.40 × 0.25
Crystal system	Triclinic	Hexagonal	Monoclinic	Trigonal	Monoclinic
Space group	$P\bar{1}$ (No. 2)	$P6_3/m$ (No. 176)	$P2_1/c$ (No. 14)	$R\bar{3}$ (No. 146)	$P2_1/n^a$
$a/\text{Å}$	12.2968(11)	9.3209(9)	14.8482(8)	17.1523(3)	11.5080(5)
$b/\text{Å}$	13.0128(12)		14.8803(8)		17.2076(7)
$c/\text{Å}$	13.7299(12)	11.143(2)	23.9239(13)	9.2856(4)	16.6511(7)
$\alpha/^\circ$	104.2431(15)				
$\beta/^\circ$	100.4996(14)		94.4133(10)		90.3365(7)
$\gamma/^\circ$	95.9048(14)				
$V/\text{Å}^3$	2068.5(3)	838.4(2)	5270.2(5)	2365.84(12)	3297.3(2)
Z	2	2	4	3	4
$\rho_{\text{calcd}}/\text{g cm}^{-3}$	1.215	1.748	1.315	1.337	1.307
μ/mm^{-1}	0.261	7.404	0.451	0.703	0.674
Temperature/ $^\circ\text{C}$	−80	−80	−80	−80	−80
Max. $2\theta/^\circ$	52.78	52.72	52.78	52.70	52.78
Total data collected	10365	3156	40529	5046	21617
Unique data, R_{int}	8299, 0.0256	608, 0.0341	10791, 0.0342	2083, 0.0167	6733, 0.0191
Obsd data [$I \geq 2\sigma(I)$]	5997	519	9105	2080	6370
Restraints/params	0/451	0/38	0/587	0/105	0/299
$S(F^2)$ [all data] ^b	1.007	1.145	1.035	1.108	1.064
$R_1(F)$ [$I \geq 2\sigma(I)$] ^c	0.0461	0.0254	0.0310	0.0178	0.0210
$wR_2(F^2)$ [all data] ^d	0.1260	0.0575	0.0831	0.0445	0.0587
$\Delta_{\text{max}}, \Delta_{\text{min}}/e \text{ Å}^{-3}$	0.443, −0.399	0.371, −0.359	0.520, −0.426	0.316, −0.228	0.358, −0.350

^a An alternate setting of $P2_1/c$ (No. 14). ^b $S = [\sum w(F_o^2 - F_c^2)^2 / (n - p)]^{1/2}$ (n = number of data; p = number of parameters varied; $w = [\sigma^2(F_o^2) + (a_0P)^2 + a_1P]^{-1}$ where $P = [\text{Max}(F_o^2, 0) + 2F_c^2]/3$; for **3b**, $a_0 = 0.0731$, $a_1 = 0$; for **6b**, $a_0 = 0.0174$, $a_1 = 0.5075$; for **8a**, $a_0 = 0.0427$, $a_1 = 2.3909$; for **10a**, $a_0 = 0.0243$, $a_1 = 0.8197$; for **10b**, $a_0 = 0.0306$, $a_1 = 1.4152$). ^c $R_1 = \sum ||F_o| - |F_c|| / \sum |F_o|$. ^d $wR_2 = [\sum w(F_o^2 - F_c^2)^2 / \sum w(F_o^4)]^{1/2}$.

For crystallographic data in CIF or other electronic format see DOI: 10.1039/b516127d

Acknowledgements

Financial support for this work was provided by the NSERC of Canada (operating grants to L.R. and a postgraduate scholarship to D.M.F.) and start-up grants from the University of Manitoba and the University of Victoria. We thank Chris Greenwood (University of Victoria) for obtaining spectra on the Bruker Avance 500 NMR spectrometer.

References

- (a) J. C. Hierso, R. Amardeil, E. Bentabet, R. Broussier, B. Gautheron, P. Meunier and P. Kalck, *Coord. Chem. Rev.*, 2003, **236**, 143–206; (b) F. A. Cotton and B. Hong, *Prog. Inorg. Chem.*, 1992, **40**, 179; (c) H. A. Mayer and W. C. Kaska, *Chem. Rev.*, 1994, **94**, 1239–1272; (d) L. Sacconi and F. Mani, *Transition Met. Chem.*, 1982, **8**, 179–252; (e) R. Mason and D. W. Meek, *Angew. Chem., Int. Ed. Engl.*, 1978, **17**, 183–194.
- The tripod 1,1,1-tris(diphenylphosphinomethyl)ethane is also sometimes referred to as “tpdme”. The linear tridentate phosphine bis(2,2'-diphenylphosphinoethyl)phenyl phosphine has also been called “triphos”, but in this article we use this name only in reference to the tripodal ligand **1**.
- C. Bianchini, A. Meli, M. Peruzzini, F. Vizza and F. Zanobini, *Coord. Chem. Rev.*, 1992, **120**, 193–208.
- Examples of tripods with non-carbon apical groups include: (a) S. Herold, A. Mezzetti, L. M. Venanzi, A. Albinati, F. Lianza, T. Gerfin and V. Gramlich, *Inorg. Chim. Acta*, 1995, **235**, 215–231; (b) T. G. Gardner and G. S. Girolami, *Organometallics*, 1987, **6**, 2551–2556; (c) L. Turculet, J. D. Feldman and T. D. Tilley, *Organometallics*, 2004, **23**, 2488–2502; (d) D. M. Jenkins, A. J. Di Bilio, M. J. Allen, T. A. Betley and J. C. Peters, *J. Am. Chem. Soc.*, 2002, **124**, 15336–15350.
- Examples of tripods with varied apical substituents include: (a) C. Bianchini, P. Frediani and V. Sernau, *Organometallics*, 1995, **14**, 5458; (b) R. A. Findeis and L. H. Gade, *Eur. J. Inorg. Chem.*, 2003, 99–110; (c) P. Schober, R. Soltke, G. Huttner, L. Zsolnai and K. Heinze, *Eur. J. Inorg. Chem.*, 1998, 1407–1415.
- Examples of tripods with a range of substituents at phosphorus include: (a) A. M. Arif, J. G. Hefner, R. A. Jones and B. R. Whittlesey, *Inorg. Chem.*, 1986, **25**, 1080–1084; (b) O. Walter, T. Klein, G. Huttner and L. Zsolnai, *J. Organomet. Chem.*, 1993, **458**, 63–81; (c) H. Heidel, J. Scherer, A. Asam, G. Huttner, O. Walter and L. Zsolnai, *Chem. Ber.*, 1995, **128**, 293–301; (d) C. Becker, L. Dahlenburg and S. Kerstan, *Z. Naturforsch., B: Chem. Sci.*, 1993, **48**, 577–582; (e) M. Sulu, L. M. Venanzi, T. Gerfin and V. Gramlich, *Inorg. Chim. Acta*, 1998, **270**, 499–510.
- Y. M. Yao, C. J. A. Daley, R. McDonald and S. H. Bergens, *Organometallics*, 1997, **16**, 1890–1896.
- A. G. Avent, D. Bonafoux, C. Eaborn, S. K. Gupta, P. B. Hitchcock and J. D. Smith, *J. Chem. Soc., Dalton Trans.*, 1999, 831–834.
- (a) D. M. Friesen, R. McDonald and L. Rosenberg, *Can. J. Chem. / Rev. Can. Chim.*, 1999, **77**, 1931–1940; (b) A comprehensive computational investigation of the conformational preferences of this tripodal system has since been published: C. A. Morrison, D. W. H. Rankin, H. E. Robertson, C. Eaborn, A. Farook, P. B. Hitchcock and J. D. Smith, *J. Chem. Soc., Dalton Trans.*, 2000, 4312–4322.
- Relative sensitivities of **3–4** to solvolysis of the P–Si bond and to oxidation at P are described in detail in the ESI†.
- B. C. Janssen, A. Asam, G. Huttner, V. Sernau and L. Zsolnai, *Chem. Ber.*, 1994, **127**, 501–506.
- Details of this variable temperature NMR study and proposed mechanisms for phosphine exchange in **3b** are included in the ESI†.
- Among structurally characterized κ^2 -triphos complexes, the six-member chelate ring has been found in both chair and boat conformations, but the former is more common. (a) R. M. Kirchner, R. G. Little, K. D. Tau and D. W. Meek, *J. Organomet. Chem.*, 1978, **149**, C15–C18; (b) D. H. Gibson, H. Y. He and M. S. Mashuta, *Organometallics*,

- 2001, **20**, 1456–1461; (c) S. C. Lin, C. P. Cheng, T. Y. Lee, T. J. Lee and S. M. Peng, *Acta Crystallogr., Sect. C: Cryst. Struct. Commun.*, 1986, **42**, 1733–1736; (d) W. O. Siegl, S. J. Lapporte and J. P. Collman, *Inorg. Chem.*, 1973, **12**, 674–677; (e) R. B. King and A. Efraty, *Inorg. Chem.*, 1969, **8**, 2374.
- 14 The κ^2 -(**3a**) Mo(CO)₄ complex was previously reported to have been prepared from the addition of **3a** to Mo(CO)₆ (ref. 8), but our attempts to repeat this synthesis using **3a** or **3b** gave only intractable tan powders, which we presume to be polymers consisting of multiple Mo centres linked by μ - κ^1 or μ - κ^2 tripodal ligands.
- 15 F. A. Cotton, *Inorg. Chem.*, 1964, **3**, 702.
- 16 A. Tarassoli, H. J. Chen, V. S. Allured, T. G. Hill, R. C. Haltiwanger, M. L. Thompson and A. D. Norman, *Inorg. Chem.*, 1986, **25**, 3541–3544.
- 17 A. Muth, O. Walter, G. Huttner, A. Asam, L. Zsolnai and C. Emmerich, *J. Organomet. Chem.*, 1994, **468**, 149–163.
- 18 S. J. Coles, P. G. Edwards, J. S. Fleming and M. B. Hursthouse, *J. Chem. Soc., Dalton Trans.*, 1995, 1139–1145.
- 19 P. G. Edwards, J. S. Fleming and S. S. Liyanage, *J. Chem. Soc., Dalton Trans.*, 1997, 193–197.
- 20 In the reaction of **9a** in the presence of PMe₃, crystals of the κ^3 -complex **10a** formed on the wall of the sealed NMR tube during heating. The ³¹P{¹H} NMR spectrum showed only κ^2 -complex throughout the reaction, but the intensity of these signals gradually diminished relative to the signal for free PMe₃. The crystals were isolated by decanting the original d₈-toluene solution, and their identity was confirmed by ³¹P{¹H} NMR.
- 21 After 12 h of heating at 85 °C, the **8a** sample still showed only **11a** as product (31% conversion) but the **8b** sample showed free Me-capped tripod **3b**, *cis* and *trans*-(PMe₃)₂Mo(CO)₃, and another unidentified species, along with **11b** (7%).
- 22 (a) C. Eaborn, P. B. Hitchcock and P. D. Lickiss, *J. Organomet. Chem.*, 1983, **252**, 281–288; (b) L. H. Gade, C. Becker and J. W. Lauher, *Inorg. Chem.*, 1993, **32**, 2308–2314.
- 23 B. Nicholls and M. C. Whiting, *J. Chem. Soc.*, 1959, 551.
- 24 D. J. Darensbourg and R. L. Kump, *Inorg. Chem.*, 1978, **17**, 2680–2682.
- 25 ¹H NMR spectra of compound **5b** consistently show 2–3% of SiMe-containing impurities, even after multiple fractional distillations. Analysis of the EI-MS trace for a sample of **5b** suggests that these contaminants are primarily composed of H(SiMe₂)_xH (292 *m/z*) and a compound with the general structure CH₃C{(SiMe₂)_xH}{(SiMe₂)_yH}{(SiMe₂)_zH} (*x* + *y* + *z* = 7436 *m/z*), both of which show fragmentation patterns similar to **5b**. These impurities were easily removed from derivatives of **5b** in subsequent synthetic steps.
- 26 Compounds **4a–b** are high-boiling oils that have been so far consistently contaminated with ~3–4% disubstituted tripod RC(SiMe₂PEt₂)₂(SiMe₂Br) (for R = H, δ_p –81.3; for R = CH₃, δ_p –82.6), and traces of other, unidentified SiMe-containing impurities. We continue to modify the reaction and work-up to avoid these impurities.
- 27 Microanalysis samples of **3b** were clean by ¹H NMR but this analysis was consistently low in carbon over repeated attempts, and with the use of V₂O₅ as a combustion agent. This may be due to SiC formation during the combustion process.
- 28 Solution samples of this compound consistently contain a fine suspension of intractable tan powder, which cannot be entirely removed, even when the solutions are filtered through Celite. We believe this insoluble by-product is an oligomeric or polymeric complex formed from intermolecular reaction of the unbound phosphine from the κ^2 product with itself, or with residual Mo starting material, based on the presence of two distinct carbonyl bands in the IR spectrum (KBr disk, ν_{CO} , cm⁻¹): 1923 (s) 1822 (s).
- 29 The extreme solubility of **9a–b** in pentane has precluded their purification for microanalysis. Impurities can be seen in the SiMe₂ region of the ¹H NMR ($\leq 5\%$).
- 30 (a) D. A. Kleier and G. Binsch, *J. Magn. Reson.*, 1970, **3**, 146; (b) K. Marat, *SpinWorks*, University of Manitoba, Winnipeg, MB, 2004.